

Investigating star formation in Illustris TNG galaxy mergers

B. Koncz¹, A.P. Joó¹ and S. Pintér²

¹ *Dept. of Astronomy, Eötvös Loránd University*

² *Dept. of Natural Science, University of Public Service, Hungary*

Received: June 30, 2023; Accepted: October 24, 2023

Abstract. Dwarf galaxies are the probable sources of the hot intra-cluster medium, a subject of a series of recent X-ray discoveries. Galaxy interaction trigger may lead to high star formation rates in these galaxies, that can lead to multiple core collapse supernovae and hot gas ejection. We studied the star formation rate history of merging galaxies in the IllustrisTNG 100-1, cosmological, magneto-hydrodynamic simulation focusing on mergers where one of the galaxies is a dwarf. We investigated the star formation rate and mass evolution of galaxies (progenitor), their dwarf merger companions (next progenitor) and their descendants at cosmological timescales with the use of the simulation's merger trees. We processed different merger trees testing the robustness of our method and found that the results are consistent. Our results show that properties of galaxies in the compared merger trees are identical, only small differences occur. We will present our methodology and the comparison of three different merger trees, including the mass and star formation rate history of the merging galaxies.

Key words: galaxies: evolution – galaxies: star formation – galaxies: interactions – methods: numerical

1. Introduction

One of the most accepted ideas about the Universe is that it is homogeneous and isotropic on a sufficiently large scale. But the question of the scale on which this can be stated arises more and more often (Paal et al., 1992; Balázs et al., 1999, 2015; Mészáros et al., 2000; Bagoly et al., 2003; Vavrek et al., 2008; Horváth et al., 2015; Horvath et al., 2020, 2022). IllustrisTNG (Nelson et al. (2017), Marinacci et al. (2018), Pillepich et al. (2017), Springel et al. (2017), Naiman et al. (2018)) is a suite of large volume, cosmological, gravo-magneto-hydrodynamic simulations including a comprehensive model for galaxy formation. Each TNG simulation self-consistently solves for the coupled evolution of dark matter, cosmic gas, luminous stars, and supermassive black holes from redshift $z = 127$ to 0 and generates 100 resulting snapshots from $z = 20$ to 0. We used the TNG100 run for analysis, the main high-resolution run including the full TNG physics model, which has the size of 110.73 Mpc^3 and contains more than 10 billion

resolution elements.

The recent X-ray discoveries show that dwarf galaxies are probable sources of the hot intra-cluster medium [Nath & Chiba \(1995\)](#). Galaxy interactions can trigger the star formation rate (SFR) in the merger companions [Shah et al. \(2022\)](#). These events can lead to energetic events like multiple core collapse supernovae. A series of proper observational census of star forming galaxies and their SFR led us to derive the star forming rate density (see eg. [Stickel et al. \(1998\)](#), [Tóth et al. \(2000\)](#), [Héraudeau et al. \(2004\)](#), [Madau & Dickinson \(2014\)](#)). Previous works investigating galaxy mergers SFR with IllustrisTNG: [Hani et al. \(2020\)](#) made a post-merger sample with about 28.000 galaxy between redshifts 0 and 1. They found no dependency on redshifts, but there is anti-correlation with stellar mass, and SFR is correlated with the gas fraction of the progenitors. Here we note that observational results on SFR should also consider geometrical effects, i.e. the attenuation of UV radiation depends also on the inclination of the disk of star forming galaxies (see eg. [Suleiman et al. \(2022\)](#)). [Patton et al. \(2020\)](#) analyzed the massive galaxies dependence on the closest companions, they found that the specific SFR is boosted by 14.5%. [Brown et al. \(2023\)](#) examined the sSFR at $z < 0.2$ as a function of the separation from the closest companion galaxy. They found that star forming galaxies show enhanced sSFR regardless of the companions' type and if there is a close passive companion, the main galaxy is likely to be a passive galaxy as well. Using the IllustrisTNG simulation other aspects of galaxy mergers were examined, e.g. supermassive black hole accretion rates in post-merger galaxies [Byrne-Mamahit et al. \(2022\)](#) and quenching in post-merger galaxies [Quai et al. \(2021\)](#).

Our goal is to estimate the differences of the galaxies average mass and SFR between the merger trees in the IllustrisTNG simulation compared to the predictions of observational uncertainties. [D'Silva et al. \(2023\)](#) used two galaxy formation simulations, Flares [Lovell et al. \(2021\)](#), [Vijayan et al. \(2021\)](#) and Shark [Lagos et al. \(2018\)](#) to explore how well the James Webb Space Telescope (JWST) [Gardner et al. \(2006\)](#) will be able to uncover the existence and parameters of galaxies at $5 < z < 10$. They found that the 1σ uncertainties by Flares are growing with z , by SFR from 0.71 to 0.98 by mass from 0.72 to 1.49 on logarithmic scale. With Shark these values are respectively between 0.32-1.03 and 0.4-1.38.

2. Method

We used the IllustrisTNG 100-1 merger tree, which is a data structure of the galaxies evolution. It uses the Sublink algorithm [Rodriguez-Gomez et al. \(2015\)](#) for the descendants search with the following steps: first the it identifies the candidates for every subhalo, it searches for galaxies in the following snapshot with common particles of the chosen galaxy. The second step is scoring of the candidates based on a merit function, which calculates the binding energy rank of each particle in the galaxies. The last step is the identification of the unique

descendant, which will be the subhalo with the highest score. To build up the merger tree, a linked-list structure was created by [Springel et al. \(2005\)](#), so that each subhalo is assigned pointers to 'key' subhalos. The 'descendant' is the unique descendant of the subhalo in question. The 'next progenitor' is the subhalo, which shares the same descendant as the subhalo in question, and which has the next largest 'mass history' behind the progenitor. In our case the progenitor galaxies are those subhalos for which the descendants and next progenitors were sorted out.

In general the progenitor galaxies are in the same snapshot, the descendants are in the following. But there are some cases, when the descendant galaxy is skipping a snapshot, or the next progenitor and the progenitor galaxies are in different snapshots. These connections between the galaxies build up the merger trees, which are completely independent from each other. Because of this independency we compared three merger trees to find out if there is any difference between them.

For analysing the data of the merger trees we downloaded the sublink tree files, which are in 20 independent files, and each of them contains about 25 million galaxies. We made a galaxy sample with star formation rates greater than 0 to reduce our sample only on those galaxies which are connected to the star formation. After making this sample we searched for the progenitor and next progenitor galaxies which have the same descendant. Since the next progenitor galaxies are less massive galaxies than the progenitors we can identify them as dwarf galaxies, in the next section at the investigation of their mass we can conclude that this assumption was correct. After that we sorted them for every redshift for $z < 15$. We didn't take into account the galaxies at higher redshift, because there were only a few of them. To avoid the problem with the snapshot skipping galaxies and those progenitors which are at different snapshots we made simplifications. Our goal is to examine the average values of large number of galaxies, therefore we simplified the galaxies snapshot numbers. We calculated the average values as if the two progenitors were in the same snapshot and their descendants in the following. We focused on two parameters of the galaxies: SFR and mass. We calculated the mean values for every snapshot ($z < 15$) for progenitors, next progenitors and descendants. We made this process for three different merger trees, the 0th, 5th and 6th, which we chose randomly from the 20 possible files.

3. Results

3.1. Mass

We first investigate the mass of the progenitor, next progenitor and descendant galaxies in a single merger tree. Fig.1 shows the average mass of the galaxies on logarithmic scale in $10^{10}M_{\odot}/h$ values, where h is the reduced hubble constant ($h = 0.6774$), at every redshift lower than 15. Each point represents the average values of the galaxies, 'X' shows the descendants, triangles the selected progenitors and squares the next progenitors. The mean mass of the descendant galaxies shows large increase especially at $z < 2$. The descendant galaxies mass are 2 order of magnitude higher at $z = 0$ than the progenitors. In general the average values of the next progenitor galaxies are lower than $10^9M_{\odot}/h$, which means that these are dwarf galaxies.

The merger tree in the IllustrisTNG 100-1 simulation contains 20 different merger trees, which are numbered from 0 to 19. We investigated three merger trees, Fig. 2 shows the comparison of these trees descendant galaxies average mass at different redshifts below 15. We examined the 0. marked with 'X', 5. 'square' and 6. 'triangle' merger tree. As the results are showing, there is no significant difference between the individual merger trees. Fig. 3 shows the logarithmic difference of the descendant galaxies average mass between the merger trees. The values are compared to the 5th merger tree's results therefore the 5th mergers values are equal to 0. There is only a slight difference (smaller than 0.1) between the trees at high redshifts $z > 2$. After $z = 2$ these differences are getting higher, especially as $z < 1$, where the 0th tree has values over 0.9 and the 6th tree about 0.6. This shows that at high redshifts the results are similar, but at $z < 2$ the dispersion is higher.

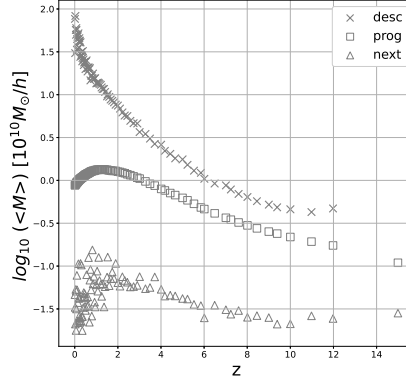


Figure 1. Merger galaxies mean mass ($\langle M \rangle$) versus redshift (z). Each dot shows the average mass versus redshift at a given Snapshot. We represented the selected progenitor galaxies with squares, next progenitors 'next' galaxies with triangles and the descendant 'desc' galaxies with 'X' markers. The progenitors and next progenitors average mass are 2-3 order of magnitude smaller than the Descendant galaxies average mass.

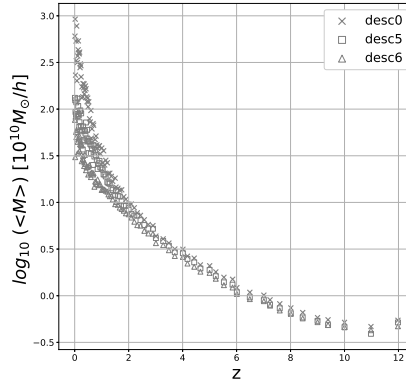


Figure 2. Comparing three merger trees descendant galaxies average mass. No significant difference can be seen between the individual merger trees, which are marked with 'X', triangle and square.

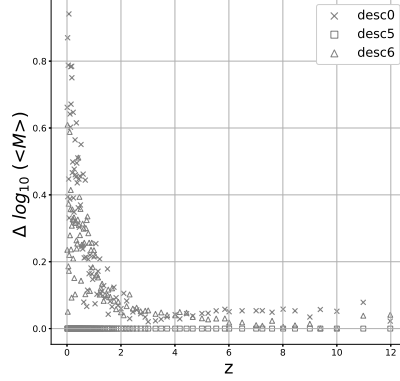


Figure 3. Logarithmic difference ($\Delta \log_{10}(\langle M \rangle)$) versus redshift (z) between the three merger trees descendant galaxies average mass. The individual trees are marked with 'X' (0th tree), square (5th tree) and triangle (6th tree). The differences are below 0.1 at $z > 2$, at lower redshifts the values are getting higher.

3.2. Star formation rate

After the masses we investigated the SFR values of the galaxies. Fig. 4 illustrates the average SFR of the galaxies in the 6. merger tree on logarithmic scale in M_{\odot}/yr values at every redshift lower than 15. Each point represents the average values of the galaxies, 'X' shows the descendants, triangles the selected progenitors and squares the next progenitors. A significant increase can be seen for every redshift between the progenitors and the descendants. Fig. 5 shows the comparing of the descendant galaxies SFR from the examined merger trees. The markers are similar to Fig. 2. The results from the trees are similar, Fig. 6 shows the logarithmic difference between them. Most of the values are below 0.4, only at $z < 1$ are some points with higher differences. Compared to the masses, the differences are in general higher ($z > 1$) and inconsistent, there is a peak at around $z = 6$ with $\Delta = 0.4$ but at $z = 2$ they are smaller than 0.2.

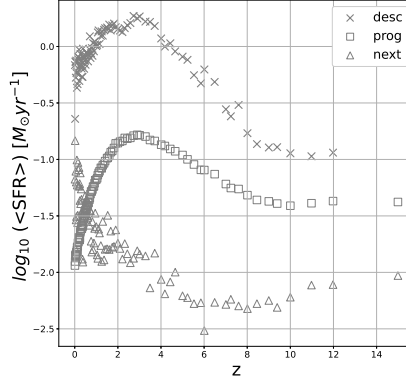


Figure 4. Merger galaxies average star formation rate ($\langle SFR \rangle$) on logarithmic scale versus redshift (z). Each point represents the average SFR of the galaxies at a given snapshot. 'X' shows the descendants, triangles the selected progenitors and squares the next progenitors. The descendant galaxies SFR is significantly higher for the whole timescale than the progenitor galaxies.

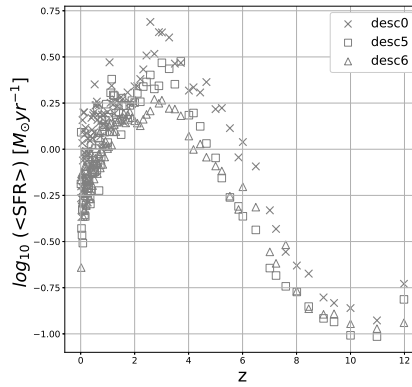


Figure 5. Comparing three merger trees descendant galaxies average SFR. No significant difference can be seen between the individual merger trees. Each mark represents the average SFR of the galaxies at a given snapshot. 'X', triangles and squares are showing an individual merger tree.

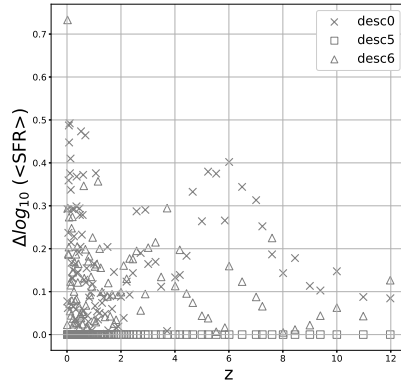


Figure 6. Logarithmic difference ($\Delta \log_{10}(\langle SFR \rangle)$) versus redshift (z) between the three merger trees descendant galaxies average SFR. The individual trees are marked with 'X' (0th tree), square (5th tree) and triangle (6th tree). Excluding one point the differences are lower than 0.5 order of magnitude at all redshifts.

4. Summary and Discussion

We investigated SFR and mass history of the merger galaxies in the IllustrisTNG simulation. We compared the average masses and star formation rates versus redshift in three individual merger tree in the simulation. We found that the descendant galaxies masses are similar at high redshifts: the logarithmic differences (Δ) are below 0.1 at $z > 2$, at lower redshifts $z < 2$ the values are getting higher $\Delta < 1$. The difference of the star formation rates are inconsistent with the redshifts. In general the values at higher redshifts are higher than by the masses (up to 0.4), but the difference at lower redshifts is smaller (up to 0.5). Compared to the simulated JWST observational data from $z = 5$ to $z = 10$, most of the uncertainties are higher than the differences between the merger trees, from which we can conclude that the individual merger trees are precise enough to examine the average properties of the galaxies at high redshifts.

To sum up, we found that there is no significant difference between the individual merger trees at higher redshifts, larger differences can occur at $z < 1$.

Acknowledgements.

We are grateful to L. Viktor Tóth for his supervision of this work and to the High Energy Astronomy Research Team (HEART - https://physics.elte.hu/KRFT_heart) for their support and thoughtful feedback.

The IBWS conference participation of B Koncz was subsidized by the Talent Support Council of ELTE Eötvös Loránd University, Budapest.

The authors thank the Hungarian TKP2021-NVA-16 and OTKA K-146092 program for their support.

References

- Bagoly, Z., Csabai, I., Mészáros, A., et al., Gamma photometric redshifts for long gamma-ray bursts. 2003, *Astronomy and Astrophysics*, **398**, 919, DOI: 10.1051/0004-6361:20021724
- Balázs, L. G., Bagoly, Z., Hakkila, J. E., et al., A giant ring-like structure at $0.78 < z < 0.86$ displayed by GRBs. 2015, *Monthly Notices of the RAS*, **452**, 2236, DOI: 10.1093/mnras/stv1421
- Balázs, L. G., Mészáros, A., Horváth, I., & Vavrek, R., An intrinsic anisotropy in the angular distribution of gamma-ray bursts. 1999, *Astronomy and Astrophysics, Supplement*, **138**, 417, DOI: 10.1051/aas:1999290
- Brown, W., Patton, D. R., Ellison, S. L., & Faria, L., Interacting galaxies in the IllustrisTNG simulations – V. Comparing the influence of star-forming versus passive companions. 2023, *Monthly Notices of the Royal Astronomical Society*, **522**, 5107, DOI: 10.1093/mnras/stad1314
- Byrne-Mamahit, S., Hani, M. H., Ellison, S. L., Quai, S., & Patton, D. R., Interacting galaxies in the IllustrisTNG simulations - IV: enhanced supermassive black hole accretion rates in post-merger galaxies. 2022, *Monthly Notices of the Royal Astronomical Society*, **519**, 4966, DOI: 10.1093/mnras/stac3674
- D’Silva, J. C. J., Lagos, C. D. P., Davies, L. J. M., Lovell, C. C., & Vijayan, A. P., Unveiling the main sequence of galaxies at $z \geq 5$ with the JWST: predictions from simulations. 2023, *Monthly Notices of the RAS*, **518**, 456, DOI: 10.1093/mnras/stac2878
- Gardner, J. P., Mather, J. C., Clampin, M., et al., The James Webb Space Telescope. 2006, *Space Science Reviews*, **123**, 485, DOI: 10.1007/s11214-006-8315-7
- Hani, M. H., Gosain, H., Ellison, S. L., Patton, D. R., & Torrey, P., Interacting galaxies in the IllustrisTNG simulations – II: star formation in the post-merger stage. 2020, *Monthly Notices of the Royal Astronomical Society*, **493**, 3716, DOI: 10.1093/mnras/staa459
- Héraudeau, P., Oliver, S., del Burgo, C., et al., The European Large Area ISO Survey - VIII. 90- μm final analysis and source counts. 2004, *Monthly Notices of the RAS*, **354**, 924, DOI: 10.1111/j.1365-2966.2004.08259.x
- Horváth, I., Bagoly, Z., Hakkila, J., & Tóth, L. V., New data support the existence of the Hercules-Corona Borealis Great Wall. 2015, *Astronomy and Astrophysics*, **584**, A48, DOI: 10.1051/0004-6361/201424829

- Horvath, I., Racz, I. I., Bagoly, Z., Balázs, L. G., & Pinter, S., Does the GRB Duration Depend on Redshift? 2022, *Universe*, **8**, 221, DOI: 10.3390/universe8040221
- Horvath, I., Szécsi, D., Hakkila, J., et al., The clustering of gamma-ray bursts in the Hercules-Corona Borealis Great Wall: the largest structure in the Universe? 2020, *Monthly Notices of the RAS*, **498**, 2544, DOI: 10.1093/mnras/staa2460
- Lagos, C. d. P., Tobar, R. J., Robotham, A. S. G., et al., Shark: introducing an open source, free, and flexible semi-analytic model of galaxy formation. 2018, *Monthly Notices of the RAS*, **481**, 3573, DOI: 10.1093/mnras/sty2440
- Lovell, C. C., Vijayan, A. P., Thomas, P. A., et al., First Light And Reionization Epoch Simulations (FLARES) - I. Environmental dependence of high-redshift galaxy evolution. 2021, *Monthly Notices of the RAS*, **500**, 2127, DOI: 10.1093/mnras/staa3360
- Madau, P. & Dickinson, M., Cosmic Star-Formation History. 2014, *Annual Review of Astron and Astrophys*, **52**, 415, DOI: 10.1146/annurev-astro-081811-125615
- Marinacci, F., Vogelsberger, M., Pakmor, R., et al., First results from the IllustrisTNG simulations: radio haloes and magnetic fields. 2018, *Monthly Notices of the Royal Astronomical Society*, DOI: 10.1093/mnras/sty2206
- Mészáros, A., Bagoly, Z., & Vavrek, R., On the existence of the intrinsic anisotropies in the angular distributions of gamma-ray bursts. 2000, *Astronomy and Astrophysics*, **354**, 1
- Naiman, J. P., Pillepich, A., Springel, V., et al., First results from the IllustrisTNG simulations: a tale of two elements – chemical evolution of magnesium and europium. 2018, *Monthly Notices of the Royal Astronomical Society*, **477**, 1206, DOI: 10.1093/mnras/sty618
- Nath, B. B. & Chiba, M., Dwarf Galaxies and the Origin of the Intracluster Medium. 1995, *Astrophysical Journal*, **454**, 604, DOI: 10.1086/176514
- Nelson, D., Pillepich, A., Springel, V., et al., First results from the IllustrisTNG simulations: the galaxy colour bimodality. 2017, *Monthly Notices of the Royal Astronomical Society*, **475**, 624, DOI: 10.1093/mnras/stx3040
- Paal, G., Horvath, I., & Lukacs, B., Inflation and compactification from galaxy redshifts? 1992, *Astrophysics and Space Science*, **191**, 107, DOI: 10.1007/BF00644200
- Patton, D. R., Wilson, K. D., Metrow, C. J., et al., Interacting galaxies in the IllustrisTNG simulations - I: Triggered star formation in a cosmological context. 2020, *Monthly Notices of the Royal Astronomical Society*, **494**, 4969, DOI: 10.1093/mnras/staa913
- Pillepich, A., Nelson, D., Hernquist, L., et al., First results from the IllustrisTNG simulations: the stellar mass content of groups and clusters of galaxies. 2017, *Monthly Notices of the Royal Astronomical Society*, **475**, 648, DOI: 10.1093/mnras/stx3112
- Quai, S., Hani, M. H., Ellison, S. L., Patton, D. R., & Woo, J., Interacting galaxies in the IllustrisTNG simulations – III. (The rarity of) quenching in post-merger galaxies. 2021, *Monthly Notices of the Royal Astronomical Society*, **504**, 1888, DOI: 10.1093/mnras/stab988

- Rodriguez-Gomez, V., Genel, S., Vogelsberger, M., et al., The merger rate of galaxies in the Illustris simulation: a comparison with observations and semi-empirical models. 2015, *Monthly Notices of the RAS*, **449**, 49, DOI: 10.1093/mnras/stv264
- Shah, E. A., Kartaltepe, J. S., Magagnoli, C. T., et al., Investigating the Effect of Galaxy Interactions on Star Formation at $0.5 < z < 3.0$. 2022, *The Astrophysical Journal*, **940**, 4, DOI: 10.3847/1538-4357/ac96eb
- Springel, V., Pakmor, R., Pillepich, A., et al., First results from the IllustrisTNG simulations: matter and galaxy clustering. 2017, *Monthly Notices of the Royal Astronomical Society*, **475**, 676, DOI: 10.1093/mnras/stx3304
- Springel, V., White, S. D. M., Jenkins, A., et al., Simulations of the formation, evolution and clustering of galaxies and quasars. 2005, *Nature*, **435**, 629, DOI: 10.1038/nature03597
- Stickel, M., Bogun, S., Lemke, D., et al., The ISOPHOT far-infrared serendipity north ecliptic pole minisurvey. 1998, *Astronomy and Astrophysics*, **336**, 116
- Suleiman, N., Noboriguchi, A., Toba, Y., et al., The statistical properties of 28 IR-bright dust-obscured galaxies and SED modelling using CIGALE. 2022, *Publications of the ASJ*, **74**, 1157, DOI: 10.1093/pasj/psac061
- Tóth, L. V., Hotzel, S., Krause, O., et al., ISOPHOT Serendipity Survey observations of interstellar clouds I. Detection of the Coldest Cores in Chamaeleon. 2000, *Astronomy and Astrophysics*, **364**, 769
- Vavrek, R., Balázs, L. G., Mészáros, A., Horváth, I., & Bagoly, Z., Testing the randomness in the sky-distribution of gamma-ray bursts. 2008, *Monthly Notices of the RAS*, **391**, 1741, DOI: 10.1111/j.1365-2966.2008.13635.x
- Vijayan, A. P., Lovell, C. C., Wilkins, S. M., et al., First Light And Reionization Epoch Simulations (FLARES) - II: The photometric properties of high-redshift galaxies. 2021, *Monthly Notices of the RAS*, **501**, 3289, DOI: 10.1093/mnras/staa3715